Life Sciences 234 (2019) 116758

Contents lists available at ScienceDirect

Life Sciences

journal homepage: www.elsevier.com/locate/lifescie

Multifunctional CuO nanoparticles with cytotoxic effects on KYSE30 esophageal cancer cells, antimicrobial and heavy metal sensing activities

Zahra Nakhaeepour[a], Mansour Mashreghi[a,b,c,*], Maryam M. Matin[a,b], Ali NakhaeiPour[d], Mohammad Reza Housaindokht[d]

[a] Department of Biology, Faculty of Science, Ferdowsi University of Mashhad, Mashhad 9177948974, Iran
[b] Novel Diagnostic and Therapeutics Research Group, Institute of Biotechnology, Ferdowsi University of Mashhad, Mashhad 9177948974, Iran
[c] Center of Nano Research, Ferdowsi University of Mashhad, Mashhad 9177948974, Iran
[d] Department of Chemistry, Faculty of Science, Ferdowsi University of Mashhad, Mashhad 9177948974, Iran

ARTICLE INFO

Keywords:
Multifunctional biogenic NPs
Fluorescent CuO
KYSE30 cell line
Anticancer properties
Antimicrobial activity

ABSTRACT

In this work, fluorescent copper oxide nanoparticles (CuO NPs) were green synthesized using viable cells, cell lysate supernatant (CLS) and protein extracts of luminescent *Vibrio* sp. VLC. Biogenic CuO NPs were then characterized by XRD, FTIR, UV/Vis spectroscopy, TEM, DLS, and PL spectroscopy. Results showed that CLS method was more efficient for CuO NPs production, therefore CuO NPs synthesized by this method from copper sulfate (CuO NPs-1) and/or copper nitrate (CuO NPs-2) were used for further studies. The crystallite size of polydispersed CuO NPs-1 and CuO NPs-2 were about 8.83 and 8.77 nm, respectively indicating their suitability for biological applications. Antibacterial activity of CuO NPs was determined using broth microdilution, well diffusion agar, and time-kill curves methods. Both CuO NP-1 and CuO NP-2 inhibited bacterial growth at the minimum inhibitory concentration (MIC) of 625 mg/L except *St. mutants* (MIC = 1250 mg/L). Emission of fluorescent light from the surface of NPs was increased when exposed to Cd^{2+}, As^{2+} and Hg^{2+} ions but decreased by Pb^{2+} ions. Results showed that CuO NP-1 had anticancer properties against KYSE30 esophageal cancer cell line (IC_{50} = 13.96 mg/L) while no higher cytotoxic effects were observed on Human Dermal Fibroblasts (HDF) (IC_{50} = 48.88 mg/L).

1. Introduction

CuO NPs production is of great value as CuO NPs have been used extensively in textiles, plastics, and paints due to their low price, high stability and high antifungal and antibacterial activities [1–3]. CuO NPs are also used in industrial fields such as gas sensors and catalytic processes [4].

CuO NPs have attracted attention mostly because of their antimicrobial, anticancer and antioxidant properties and they may be used in many other biomedical applications [5,6]. Although CuO nanoparticles may have different applications depending on the various properties they manifest, which are highly influenced by their size, surface properties, optical and magnetic traits, however, the synthesis method being an important parameter for controlling all these and thus, their biomedical and pharmaceutical properties.

Bacteria are routinely used in bioprocesses in the form of viable cells, cell lysate supernatant (CLS) and protein extracts [7]. Also, bacterial supernatants and biomass and their derived components such as proteins are three major microbiological formulas for the extracellular or intracellular biosynthesis of NPs [8]. Extracellular biosynthesis of NPs is more beneficial because it allows easier purification of NPs during the synthesis [9]. Intracellular biosynthesis of copper and copper oxide NPs have been performed using *Serratia* sp. [10], while *Salmonella typhimurium* [11], *Thermoanaerobacter* sp. X513 [7], *Escherichia coli* [12], *Pseudomonas fluorescence*, and *Pseudomonas aeruginosa* [13] were applied for extracellular processes. Several other bacteria such as *Pseudomonas stutzeri*, *Pseudomonas* sp., *Streptomyces* sp., *Lactobacillus* sp., *Morganella morganii* RP4, and *Morganella psychrotolerans* were also considered for CuO NPs synthesis in which no indication for their mode of production presented [14].

* Corresponding author at: Department of Biology, Faculty of Science, Ferdowsi University of Mashhad, Mashhad 9177948974, Iran.
E-mail addresses: mashrghi@um.ac.ir (M. Mashreghi), matin@um.ac.ir (M.M. Matin), a.nakhaei@um.ac.ir (A. NakhaeiPour), housain@um.ac.ir (M.R. Housaindokht).
URLs: http://mashreghi.profcms.um.ac.ir (M. Mashreghi), http://matin.profcms.um.ac.ir (M.M. Matin), http://a.nakhaei.profcms.um.ac.ir (A. NakhaeiPour), http://housain.profcms.um.ac.ir (M.R. Housaindokht).

https://doi.org/10.1016/j.lfs.2019.116758
Received 1 June 2019; Received in revised form 4 August 2019; Accepted 12 August 2019
Available online 14 August 2019

Luminescent bacteria have special values in biotechnology, especially in microbial biosensors construction. Application of these bacteria (naturally occurring or genetically engineered) for biosynthesis of gold and TiO_2NPs have been reported recently [15–17] however, there are not any reports for the use of such bacteria for CuO NPs biosynthesis. It is worth mentioning that oxidoreductase enzymes of these bacteria are involved in the process of luminescence illumination, and the fact that the bacterial enzymes involvement in the production of NPs seems to be very likely [15].

Basically, molecules such as enzymes, proteins, peptides, and polysaccharides within microbial cells or their growth medium are potentially appropriate candidates for biosynthesis of metallic NPs [9]. These organic materials are able to reduce metal ions to metal NPs using their functional groups, such as cysteine, histidine, aldehydes, and ketones [10]. In another hand, the large variety of proteins and peptides provides a new approach to control, organize, and direct the size, shape, and structure of metal NPs. Tan and co-workers used the 20 natural R-amino acids for synthesis of gold NPs. They showed that the pure charge and the reduction capability of the peptide have an important role in the growth and nucleation of the gold NPs [18].

In this work, simple, fast and eco-friendly approaches have been investigated for CuO NPs synthesis to obtain more appropriate NPs with anticancer, antibacterial and photoluminescence (PL) properties.

2. Materials and methods

2.1. Bacterial strains

Luminescent bacteria strains designated as VLA, VLB and VLC were previously isolated from an Iranian shrimp farm and after identification using 16s rRNA gene sequencing analysis (showing 99% similarity to *Vibrio harveyi*) have been considered in NPs biosynthesis experiments. Standard strains of *Escherichia coli* ATCC25922, *Staphylococcus aureus* ATCC25923, and *Streptococcus mutants* PTCC1683 (procured from Iranian Research Organization for Science and Technology, Tehran, Iran) were used in this study for investigation on antimicrobial activities of CuO NPs. For similar purposes, *Pseudomonas aeruginosa* was obtained from Microbiology Division of Ghaem Hospital of Mashhad University of Medical Science.

2.2. Determination of maximum tolerance concentration (MTC)

Resistance to Cu^{2+} was determined for each luminescent strains by growing them separately in Sea Water Complete medium (SWC, 2.4% w/v sea salt, 0.5% w/v peptone, 0.3% w/v yeast extract, and 0.3% v/v glycerol) (10^8 CFU/mL) with final concentration of copper sulfate ($CuSO_4.5H_2O$, Merck) from 300 to 550 mg/L. The cultures were incubated at 28 °C for 24 h. The MTC was determined by observing the presence or absence of visible growth on agar plates [19]. *Vibrio* sp. VLC was selected among other luminescent strains for CuO NPs synthesis because of exhibiting higher tolerance and better growth in the presence of copper salts.

2.3. Biological production of CuO NPs

CuO NPs were synthesized by reduction of copper sulfate and copper nitrate [Cu $(NO_3)_2{\cdot}3H_2O$, Merck] using *Vibrio* sp. VLC as reducing agents according to the three protocols that are explained in the following sections.

2.3.1. Biosynthesis of CuO NPs by viable bacterial cells

Vibrio sp. VLC were grown in Luria-Bertani (LB) broth (Merck, Germany and Himedia, India) without NaCl (1% peptone, 0.5% yeast extract, and pH 7 in distilled water) at 200 rpm, 30 °C for overnight. Then 98 mL of sterile LB was inoculated by 1 mL of fresh inoculums of bacteria (OD600 = 0.1). Thereupon 1 mL of sterile stock solution of copper salt solution was added to the reaction mixture and incubated for up to 2–5 days at 30 °C under shaking conditions (200 rpm). After the completion of the reaction, bacteria were removed by centrifugation (5000 rpm for 10 min) and the colored supernatant containing a suspension of CuO NPs was filter-separated for further analysis. Nanoparticles were purified by centrifugation of filtered solution at 140000 rpm for 1 h. Supernatants were discarded, and the precipitate was dried in a vacuum oven (Memmert, Germany) at 110 °C for 24 h before further use or analysis. Copper salt solution without bacteria and bacteria culture without copper salt solution were used as controls. No color change was observed during the test [7].

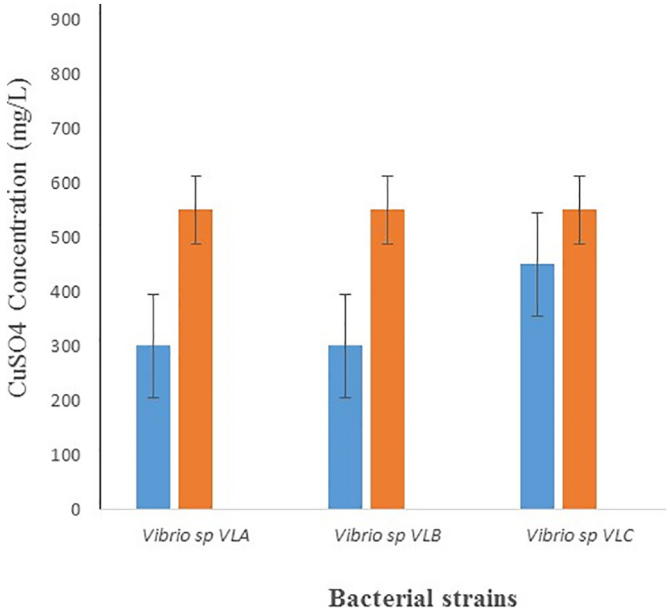

Fig. 1. Maximum tolerance concentration (MTC■) and minimum inhibitory concentration (MIC■) of $CuSO_4$ for selected luminescent strains (*Vibrio* sp. VLA, *Vibrio* sp. VLB, *Vibrio* sp. VLC).

2.3.2. Biosynthesis of CuO NPs by cell lysate supernatant (CLS)

For the preparation of cell lysate supernatant, bacteria were first grown in modified LB broth (without NaCl). The cultures were incubated at 200 rpm, 30 °C for 48 h and then centrifuged at 7500 rpm for 15 min. Obtained pellets were resuspended in sterile distilled water and sonicated with an ultrasonic processor (GM2070, Bandelin Sonopuls, Germany) for 15 min. The sonicated samples were centrifuged at 5000 rpm for 20 min. For CuO NPs production, the resultant supernatant which called CLS was incubated with 25 mM copper salt for 24 h at 30 °C and placed in the water bath (100 °C) for 1.5 h. CuO NPs were purified by centrifuging the mixture at 10,000 rpm for 30 min to collect the precipitate. The precipitate was washed with deionized water three times and dried in vacuum oven (Memmert, Germany) at 110 °C for 24 h. The products were used as CuO NPs for further characterizations. Simultaneously, two controls including the CLS of bacteria without copper salt solution and copper salt solution without CLS were maintained at the same condition [20].

2.3.3. Biosynthesis of CuO NPs by protein extract of Vibrio sp. VLC

Protein extracts of CLS from the previous procedure (2.3.2) were placed into dialysis bags. A semipermeable membrane (molecular weight cut off of 12 kDa, Sigma) was used to separate micro molecules and macromolecules based upon their size. Dialysis was carried out for two days against distilled water at a temperature of 4 °C. Then, ammonium sulfate (Merck, Germany) was added to the suspension in the bag according to the encorbio site (http://www.encorbio.com/protocols/AM-SO_4.htm) and was held for 24 h at a temperature of

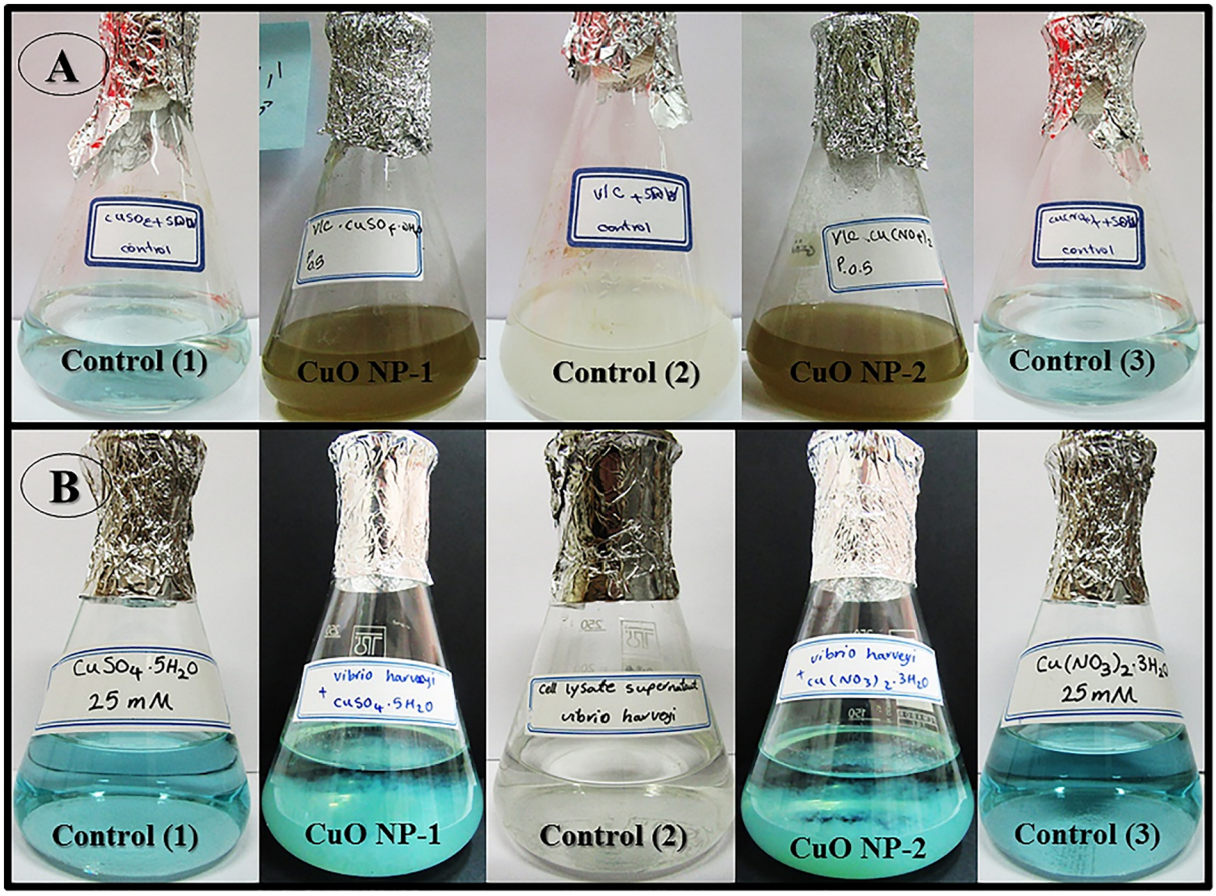

Fig. 2. Visual detection of synthesized CuO NP. A: CuO NPs synthesized using viable cells of *Vibrio* sp. VLC in the presence of copper sulfate (CuO NP-1) and copper nitrate (CuO NP-2). B: CuO NP synthesis using CLS of *Vibrio* sp. VLC in the presence of copper sulfate (CuO NP-1) and copper nitrate (CuO NP-2). As the number of changes (precipitation) for NPs biosynthesis using proteins were few and not clearly observable in images, results were not presented but confirmed by UV–visible spectroscopy (see Fig. 3). Control (1): copper sulfate without bacteria; control (2): bacteria (viable cells or CLS) without salt; control (3): copper nitrate without bacteria.

4 °C. This was done for better deposition of proteins. Protein deposits were further precipitated by 10,000 rpm centrifugation at 4 °C for 20 min. Protein precipitates were dissolved in 20 mM phosphate buffer (pH = 7) and dialyzed against phosphate buffer for 24 h [21]. When copper salt solution (25 mM) was added to the above-prepared suspension, CuO NPs as precipitate was visible at the bottom of the flask and purified powdered by drying for further use.

2.4. CuO NPs characterization

Further experiments were carried out after detection of CuO NPs, either by the formation of sediments at the bottom of the flask or changes in color from blue to dark green or brown. Therefore, the reaction mixture of CuO NPs was subjected to optical analysis and the spectra were obtained at the resolution of 1 nm from 200 to 800 nm for each sample by UV–Vis spectrophotometer (Shimadzu UV-1700, Tokyo, Japan). Then FTIR spectra (resolution of 4 cm^{-1}) were recorded from 400 to 4000 cm^{-1} on an FTIR spectrometer (Nicolet Avatar, Madison, WI, USA) at room temperature. Zeta potential can be an index to the stability of the colloidal particles. Therefore in this study, 0.001 g of the dried powder of the synthesized CuO NPs was dispersed in culture medium using an ultrasonic cleaner and the zeta potential was determined at neutral pH and 22° C using a Zeta Compact (CAD, France).

Also, XRD studies were carried out on an Explorer X-ray diffractometer instrument (GNR Analytical Instruments, Italy) using CuKα radiation (0.15418 nm). Scanning was performed with the scan angle 2θ, the scan range of 30 to 80 degrees. XRD data analysis was accomplished using MATCH software and the average size of CuO NPs was calculated by using Debye–Scherrer equation ($D = 0.9\ \lambda/\beta\ \cos\theta$), in which λ is the X-ray wavelength of Cu Kα radiation, β is the FWHM of the respective diffraction peak and θ is the Bragg diffraction angle. Furthermore, the DLS device (CordouanVASCO3, France) was used to determine the size and size distribution profile of small particles in suspension. DLS measurement was performed on the aqueous dispersion of CuO NPs through manually grinding the obtained precipitated powder in mortar dissolved in ethanol, followed by 1 h sonication. The features and shapes of the particles were imaged by transmission electron microscope (TEM) (Leo 912 AB, Germany).

2.5. Antimicrobial activity of CuO NPs

2.5.1. Minimum inhibitory concentration (MIC) and minimum bactericidal concentration (MBC) determination

MIC, is defined as the lowest concentration of the nanoparticles, inhibiting the growth of the bacteria with no significant increases [22]. A microdilution method was used to evaluate the bactericidal effects of CuO NPs. The antibacterial solutions were prepared using serial two-fold (1:2) dilutions of CuO NPs in concentrations ranging from 19.5 to 1250 mg/L within microplates wells. Then, a suspension of 1.5×10^8 CFU/mL (according to the 0.5 McFarland standard) of bacteria (*Escherichia coli* ATCC25922, *Pseudomonas aeruginosa*, *Staphylococcus aureus* ATCC25923and *Streptococcus mutants* PTCC1683) was prepared in nutrient broth (NB; Merck), diluted 20 times in buffered solution within 96 well microtiter plates and incubated at 37 °C for

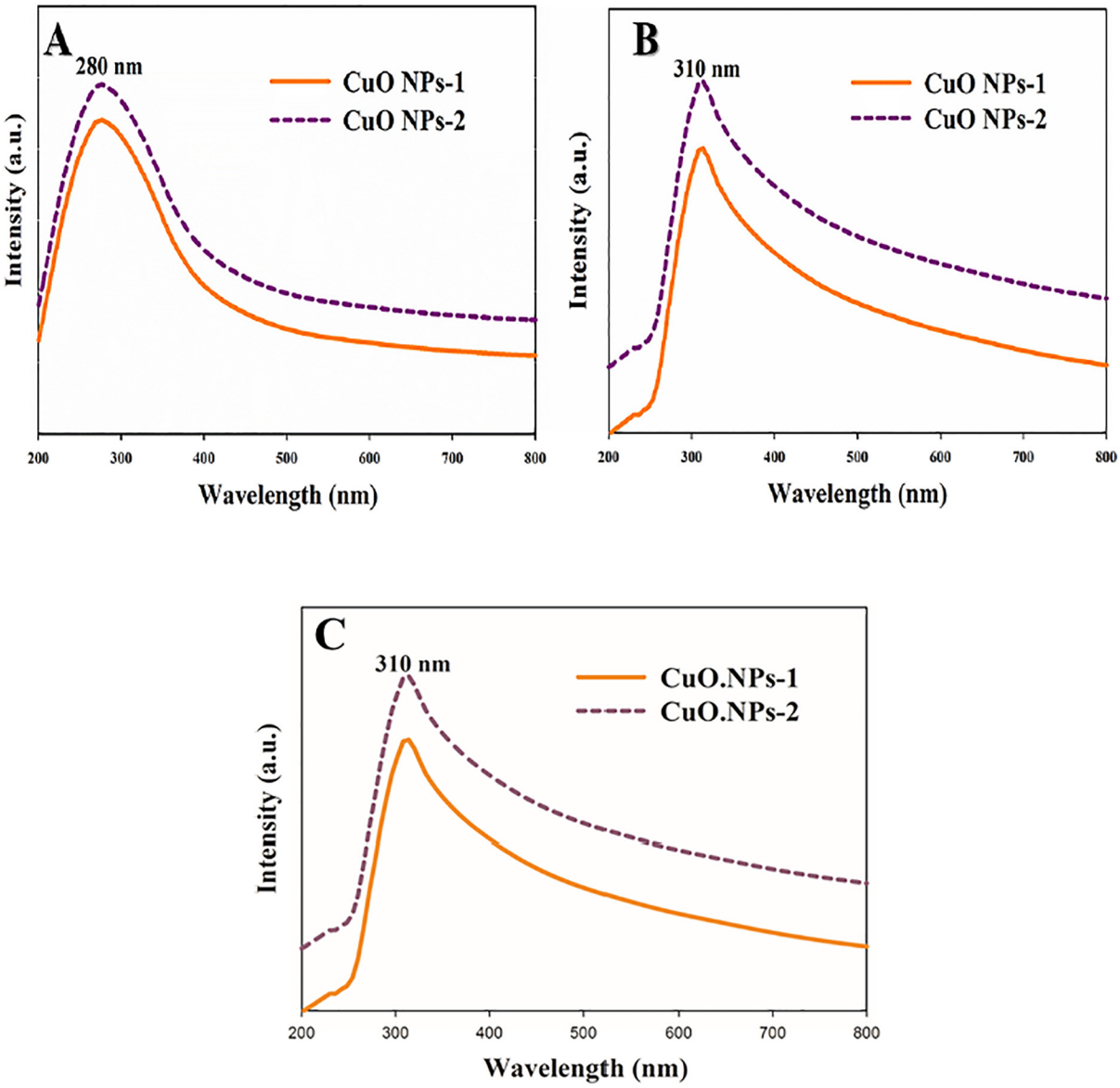

Fig. 3. UV–visible spectroscopy analysis (UV–visible spectrum) of CuO NPs synthesized by viable cells (A) CLS (B) and proteins (C) of *Vibrio* sp. VLC in the presence of copper sulfate (Solid - CuO NP-1) and copper nitrate (Dash - CuO NP-2).

24 h. In the range of sample turbidity, the MIC was determined to identify the lowest concentration of antibacterial agent that inhibits 99% of the bacterial growth. A microdilution measurement was done in triplicate to confirm the value of MIC for each tested bacterium. As such, the MBC was measured after MIC determination by pipetting 10 µL from all concentrations of CuO NPs onto nutrient agar (NA; Merck) plates further incubated at 37 °C for 24 h. The MBC endpoint was interpreted as the lowest concentration of antibacterial agent killing 100% of the initial bacterial population [23,24].

2.5.2. Well diffusion method

Bacterial inocula were sub-cultured in NB and incubated overnight at 37 °C. Then NA was swabbed with the respective subcultures of the above strains (1.5×10^8 CFU/mL). Specimens containing CuO NPs were then arranged on the swabbed agar surface and incubated at 37 °C for 24 h. The results were recorded by measuring the diameter of the inhibition zone (mm) [25].

2.5.3. Time-kill method (time-kill curve)

Different concentrations of CuO NPs were prepared as explained in the MIC experiment (Section 2.5.1). The bacterial suspension was added to the wells of a microtiter plate in the final volume of 10^4 CFU/well. To ensure the contact of the NPs with bacteria during testing, microtiter plates were placed in a shaking incubator (37 °C, 100 rpm). After inoculation, the absorbance of the sample at 630 nm was measured at intervals of 2 h. Data was recorded and plotted in the form of the growth curve. In this experiment, the dispersed NPs in the medium were used as the blank. Also, the medium and NPs without bacteria and bacterial culture without NPs were considered as controls [26].

2.5.4. Atomic force microscopy (AFM)

The effect of CuO NPs-1 on the bacterial cell surfaces was examined by AFM. CuO NPs-1 and *E. coli* were selected randomly in this section in which its results can be distributed to other NPs and bacteria. 1 mL of bacterial suspension without treatment (control) and treated with CuO NPs (with the final concentration of MIC) was prepared and diluted 20 times. Then 5 µL of prepared solution was placed on a mica surface and

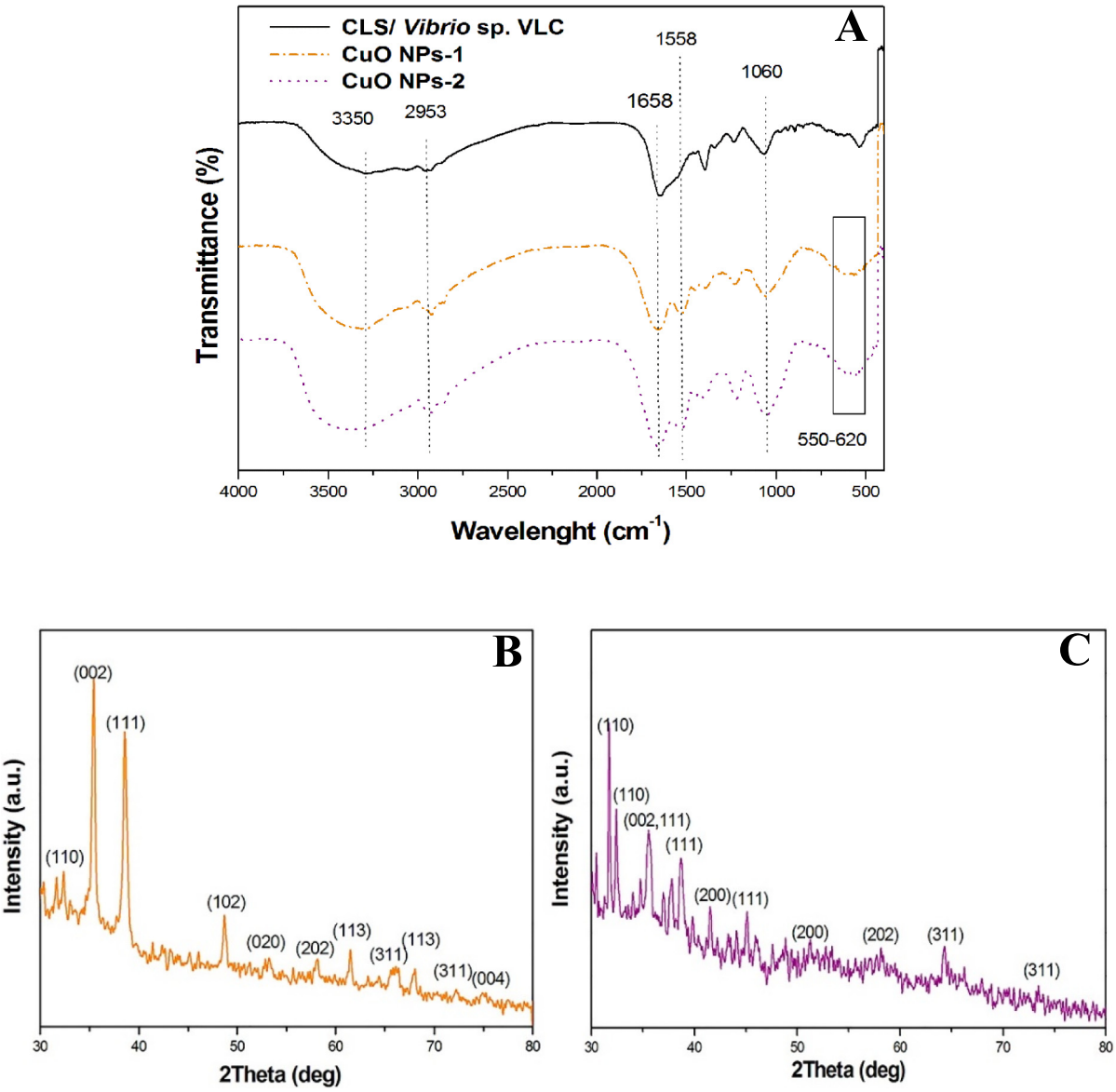

Fig. 4. FT-IR spectrum of CuO NPs (CuO NPs-1 and CuO NPs-2) (A); XRD patterns of B: CuO NP-1, and C: CuO NP-2 synthesized using CLS of *Vibrio* sp. VLC.

air dried before analysis [27]. AFM analysis was carried out with an atomic force microscope (Multi-Mode, Full model, Iran) for its detail size, morphology, and agglomeration of CuO NPs. AFM images were taken with silicon cantilevers with force constant 0.02–0.77 N/m, tip height 10–15 nm, contact mode.

2.6. Cytotoxicity study of CuO NPs

2.6.1. Cell culture and various treatments

KYSE30 cells (human esophageal squamous cell carcinoma), were obtained from Pasteur Institute (Tehran, Iran) and normal HDF cells (Human Dermal Fibroblasts, a primary cell line) were kindly provided by Academic Center for Education, Culture and Research (ACECR, Khorasan Razavi, Iran). KYSE30 cells were cultured in Roswell Park Memorial Institute medium (RPMI 1640 medium, Biowest, Nuaillé, France) supplemented with 10% fetal bovine serum (FBS; Biowest, France) [28]. HDF cells were grown in high-glucose Dulbecco's Modified Eagle's Medium (DMEM, Gibco, Paisley, UK) containing 10% FBS and 1% penicillin/streptomycin. Cells were incubated at 37 °C in a CO_2 incubator (95% air, 5% CO_2 and 100% relative humidity). To determine the half maximal inhibitory concentration (IC_{50}) of CuO NPs, cells were seeded at a density of 10,000 cells/well (for KYSE30 cell line) and 8000 cells/well (for HDF cell line) in 96-well tissue culture plates (Falcon Becton-Dickinson). Cells were grown until 70% confluency were treated with different concentrations (6.25, 12.5, 25, 50, 100 and 200 mg/L) of CuO NP-1 (selected in random) and chemically synthesized CuO NPs (US research nanomaterials Inc., 40 nm in size) dispersed in PRMI and DMEM medium by sonication (Ultrasonic Bandelin Sonopuls, Germany) and further incubated for 24, 48 and 72 h. Meanwhile, a similar procedure using the same concentrations of $CuSO_4.5H_2O$ was performed as a control on KYSE30 cells. Cisplatin (Sigma, USA) (3.75, 6.25, 12.5, 25 and 50 mg/L) was also used as a positive control.

Investigating the cellular uptake, cytoplasmic transport and distribution of NPs inside the cells provide new insight into their intracellular behavior. Therefore, to study the CuO NPs cell internalization, KYSE30 cells were incubated with 13.96 µg/ml CuO NPs-1 for 24 h, washed with PBS three times and fixed (2.5% glutaraldehyde) for 2 h. The cells were then post-fixed in 1% osmium tetroxide for 2 h, washed and dehydrated in graded concentrations of ethanol (25%, 50%, 70%, and 100%) and propylene oxide. Next, cell samples were embedded in pure resin (Araldite 502 Resin Kit) (TAAB, UK) and after complete passage of the samples and resin curing by placing the

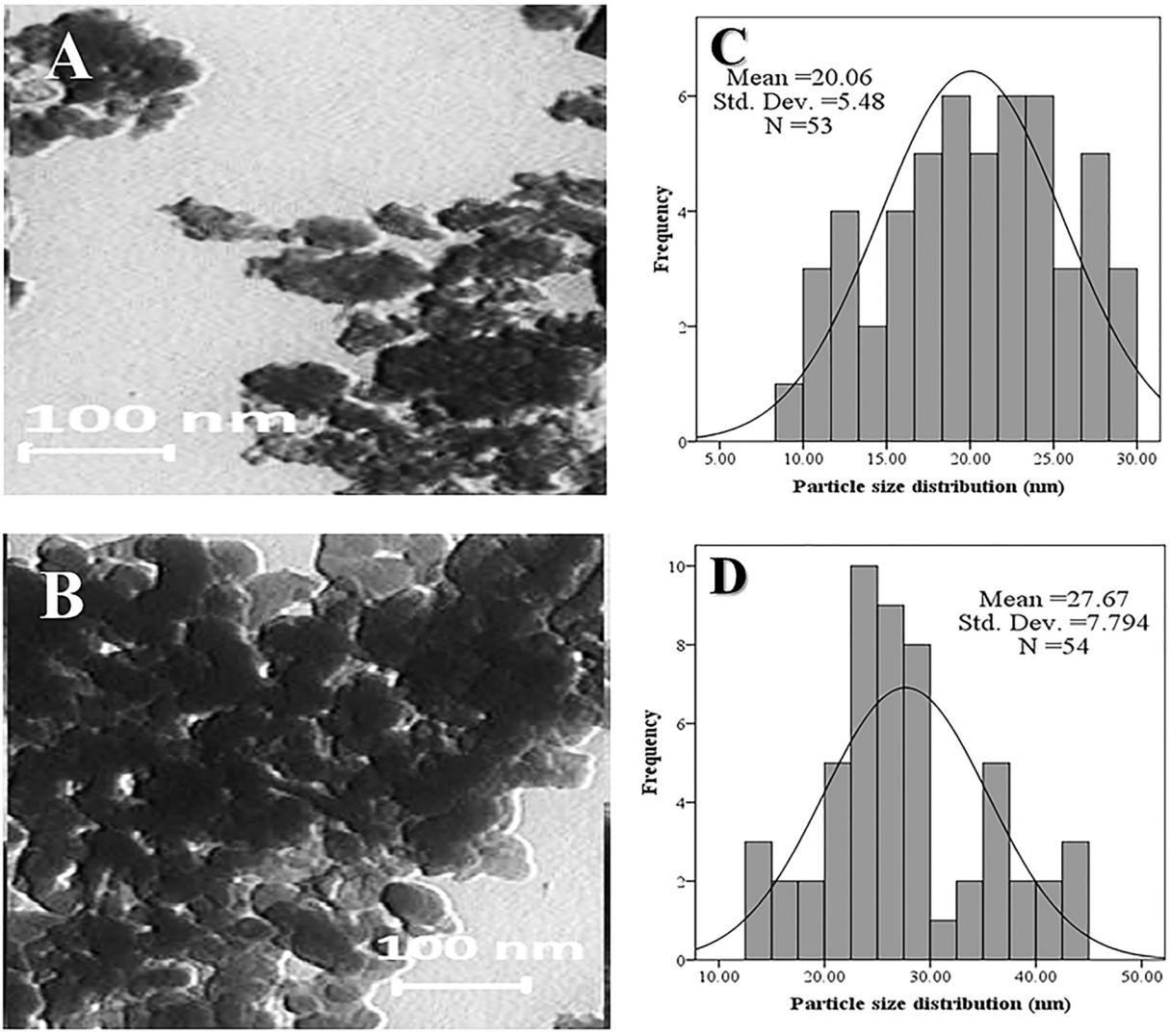

Fig. 5. TEM micrographs and the corresponding histograms of CuO NP-1 (A, C) and CuO NP-2 (B, D) synthesized using CLS of *Vibrio* sp. VLC.

capsules at 60 °C for 2 days, the blocks were first trimmed and then cut by an ultramicrotome (Leica Ultracut R, Vienna, Austria). Thin sections of 60–70 nm were collected on copper grids and visualized by TEM (Leo 912 AB, Germany).

2.6.2. MTT assay

The thiazolyl blue (MTT) assay was used to measure the cytotoxicity of CuO NPs on KYSE30 and HDF cell lines. It is a colorimetric assay for measuring cell viability. The cellular enzymes reduce the tetrazolium dye to its insoluble formazan product producing a purple color. 24, 48 and 72 h after treatments, 20 µL of MTT dye (5 mg/mL, Atocel, Austria) was added to each well of 96-well plates and incubated for 4 h at 37 °C. Then, media were replaced by dimethyl sulfoxide (DMSO, 150 µL/well) and optic densities of wells were measured at 545 nm by an ELISA microtiter plate reader (Stat fax 2100, Awareness Technology, Inc., USA). All tests were performed in triplicate, and cells were checked for morphological alterations by an inverted microscope (hp, Japan) [29]. For microscopic observation, cells were washed twice with PBS after CuO NPs containing medium was aspirated and then incubated with DMEM. The percentage of cell viability was calculated using the following formula:

$$\text{Cell viability (\%)} = (AT/AC) \times 100$$

where AT is the average absorbance of three replicates of cells treated with different concentrations of nanoparticles, and AC represents the average absorbance of three replicates of blank (medium + different concentrations of nanoparticles). Then, the logarithm of the concentrations was calculated, and the log[inhibitor] versus cell viability curves were plotted using GraphPad Prism version 6.07 for Windows (GraphPad Prism Software, La Jolla, CA, USA). IC_{50} values were calculated by nonlinear regression analysis of the mean dose–response curve for each nanoparticle.

2.7. Heavy metal sensing analysis

Photoluminescence is the spontaneous emission of light from a material under optical excitation. A suspension of CuO NPs-2 was prepared in the presence of different solvents and heavy metals (mercury, lead, arsenic, cadmium) and its emission spectrum were measured with excitation at a wavelength of 310 nm using a luminescent spectrometer (Perkin-Elmer, LS45USA). The fluorescent images were taken with a fluorescence microscope (Zeiss, Germany). The selection of CuO NPs-2 for this study was also randomized among other CuO NPs. Further studies on other CuO NPs synthesized in this research studies are encouraged.

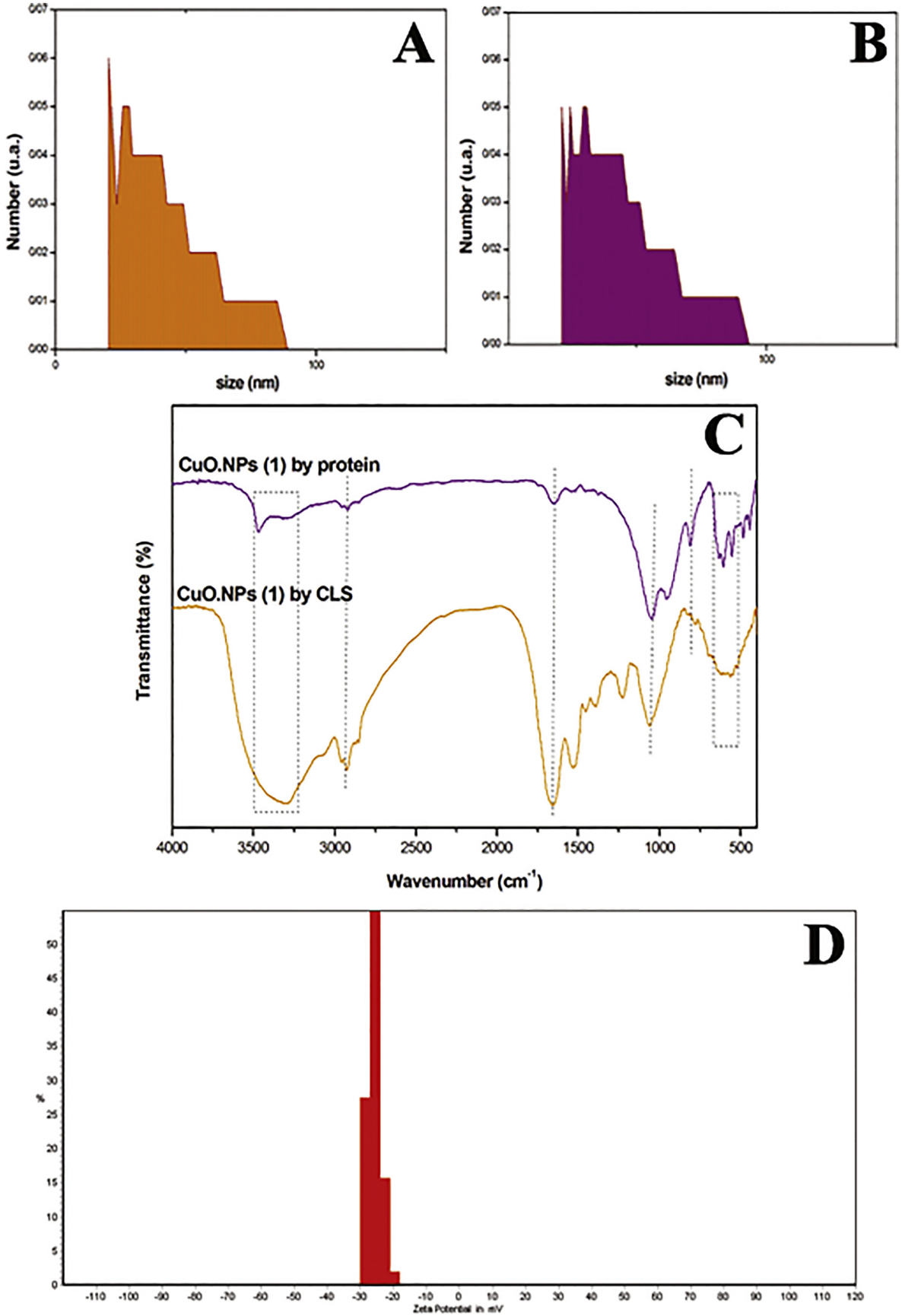

Fig. 6. Particle size distribution pattern of A: CuO NP-1 and B: CuO NP-2. C: Comparison of FTIR spectrum of CuO NPs produced by luminescent bacteria (*Vibrio* sp. VLC), and D: Zeta potential histogram of CuO NPs (−25.86 mv) indicating stability of the synthesized nanoparticles.

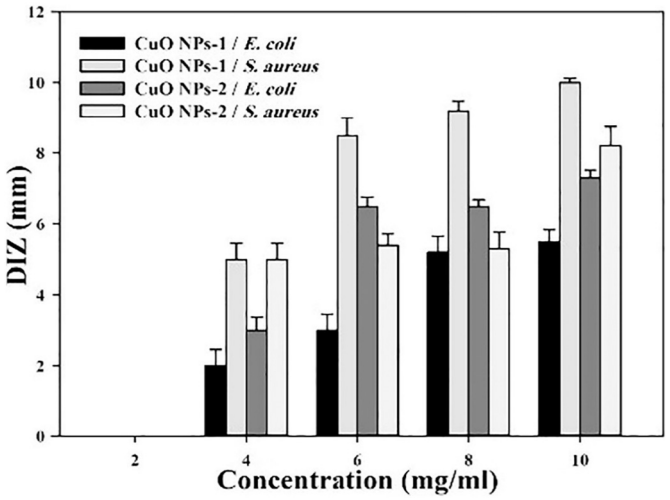

Fig. 7. The diameter of the inhibition zone (DIZ) produced by different CuO NPs (CuO NPs-1, CuO NPs-2) concentrations synthesized using CLS of *Vibrio* sp. VLC against indicator bacteria (*E. coli*, *S. aureus*). The results are shown as mean ± SD.

3. Results

3.1. Determination of maximum tolerance concentration (MTC)

The bacterial resistance to various concentrations of copper ions (300 to 850 mg/L) was determined according to bacterial growth after three days of incubation at 30 °C. *Vibrio* sp. VLC showed the highest resistance to 450 mg/L of $CuSO_4$ (Fig. 1). *Vibrio* sp. VLA and *Vibrio* sp. VLB were mostly resistant to 300 mg/L of Cu solution [30]. Therefore VLC strain was selected for further studies.

3.2. CuO NPs biosynthesis and characterization

Changes of solution color to dark green or brown and precipitation at the bottom of the flasks were a primary indication for CuO NPs biosynthesis (Fig. 2). Protein denaturation and surface tension reduction caused by increases in temperature lead to a better and faster reduction of copper ions when CLS and protein were used for NPs synthesis. However, as less protein content was obtained after dialysis not enough CuO NPs were obtained for further characterization.

The UV–visible spectrum of CuO NPs in the range of 200 to 800 nm is shown in Fig. 3. Sharp peaks at 280 nm and 310 nm are related to the production of the NPs. The bands around 3200–3600 cm^{-1} (O—H), 2953 cm^{-1} (Amin I&II), 1658 cm^{-1} and 1558 cm^{-1} (Amide I&II) in the FT-IR spectra of CLS and CuO NPs (Fig. 4A) confirmed the presence of biological agents such as proteins on the surface of the NPs. We concluded that the vibrational stretches in the 550–620 cm^{-1} belong to the band of Cu—O. In Fig. 4A, the band of 1050–1150 cm^{-1} is related to C—O stretch of alcohol [31].

XRD patterns of CuO NPs synthesized by CLS showed that all possible peaks representing CuO NPs were present, indicating the monoclinic crystal system of CuO NPs (JCPDS File No: 048-1548) (Fig. 4B and C). The crystallite size corresponding to the highest peak observed in the XRD pattern was estimated using the Debye–Scherer equation. They were 8.83 and 8.77 nm for CuO NP-1 and CuO NP-2 respectively. The presence of sharp structural peaks in XRD patterns and crystallite size < 100 nm revealed the nanocrystalline nature of CuO NPs.

TEM images and size distribution histograms of CuONPs-1 and CuO NPs-2 depicted the approximate uniform distribution of mentioned NPs with the average particles size of 20–27 nm (Fig. 5). Furthermore, DLS analysis showed a polydispersity status with the average particle size and PDI of 40 nm, 0.296 and 42 nm, 0.285 for CuONP-1 and CuO NP-2 respectively (Fig. 6A and B). FTIR analysis was used to confirm the role of protein within CLS mixture in the biosynthesis of CuO NPs (Fig. 6C). Stability of CuO NPs were examined in various solutions (distilled water, DMSO, glycerol citrate, NB medium, PRMI 1640 medium and FBS) by direct observation of NPs precipitation. It was found that except distilled water, CuO NPs were stable in all mentioned solutions for up to 72 h which was sufficient for further experiments. The zeta potential is measured to get some information on the surface charge and the stability of the colloidal suspension [32]. The colloidal suspension of the prepared CuO NPs showed a zeta potential value of −25.86 mV (Fig. 6D) indicating a good stability of nanoparticles.

3.3. Assessing the antimicrobial activity of CuO NPs

The diameter of inhibition zone (DIZ) is a reflection of microbial susceptibility magnitude that in this study enlarged with an increase of CuO NPs concentration (Fig. 7). Results of MIC and MBC showed the high sensitivity of *P. aeruginosa* (MBC = 312.5 mg/L) and high resistance of *S. mutants* (MBC = 1250 mg/L) to CuO NPs (Table 1). CuO NP-2 had higher inhibition effect on gram-negative bacteria while gram-positive growth was more prevented by CuO NP-1. The growth profile (time-kill curve) of *E. coli* and *S. aureus* strains in the presence of varying concentrations of CuO NP-1 and CuO NP-2 was also investigated [Fig. 8(A–D)]. The delay in Lag phase was observed for both bacterial strains on exposure to different concentration of both CuO NP-1 and CuO NP-2. In general, by increasing nanoparticles concentration, *S. aureus* growth was more inhibited than *E. coli*. Meanwhile, the accumulation of CuO NP-1 on *E. coli* cell surface and its effect on bacterial cell disruption was observed by AFM at 2 h and 6 h after incubation (Fig. 9).

3.4. Assessing the anticancer properties of CuO NPs

Since no significant differences were observed in NPs characteristics and antimicrobial properties between CuONP-1 and CuO NP-2, one nanoparticle (CuO NP-1) was randomly selected for further cytotoxicity studies (Fig. 10). After 24, 48 and 72 h treatment of KYSE30 and HDF cell lines with UV sterilized CuO NP-1, the viability of KYSE30 cells highly decreased [IC_{50} = 37.52 mg/L (24 h), IC_{50} = 18.26 mg/L (48 h) and IC_{50} = 13.96 mg/L (72 h)] in a dose-dependent manner in comparison to HDF normal cells [IC_{50} = 60.25 mg/L (24 h), IC_{50} = 35.9 mg/L (48 h) and IC_{50} = 48.88 mg/L (72 h)] (Fig. 10D and E). In control experiments, the effects of chemically synthesized CuO NPs (US Research Nanomaterials, Inc.), copper sulfate salt and cisplatin were also investigated on both cell lines (Fig. 10A). Results showed that KYSE30 cell survival was much lower when exposed to polydispersed biogenic CuO NP-1 compared to the copper salt solution

Table 1
MIC and MBC of CuO NPs synthesized using CLS of *Vibrio* sp. VLC against different Gram-positive and Gram-negative bacteria.

	MIC (mg/L)				MBC (mg/L)			
	E. coli	*P. aeruginosa*	*S. aureus*	*St. mutans*	*E. coli*	*P. aeruginosa*	*S. aureus*	*St. mutans*
CuO NP-1	625	312.5	625	625	625	312.5	625	1250
CuO NP-2	625	312.5	312.5	1250	625	312.5	625	1250

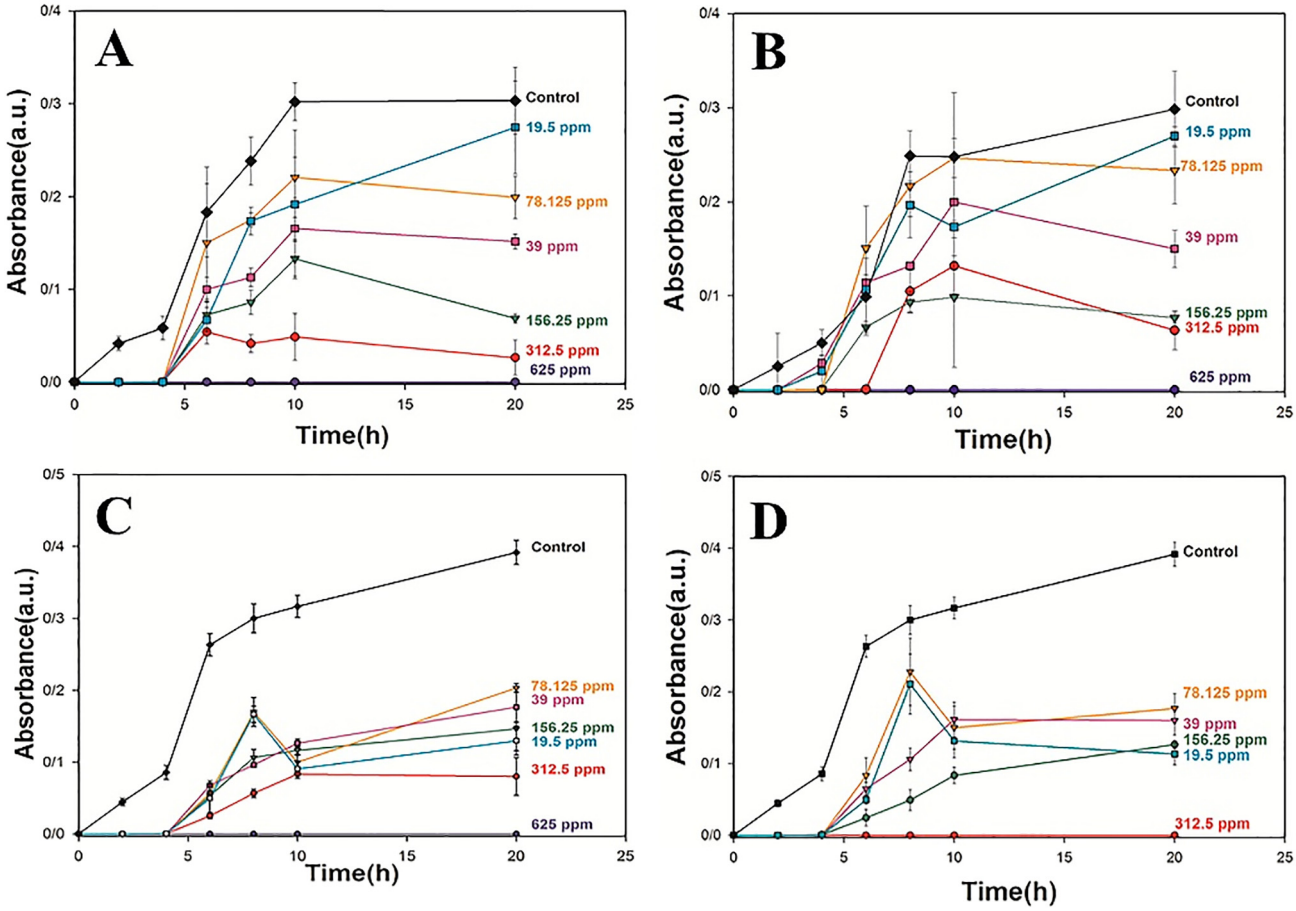

Fig. 8. Time-kill curves of CuO NPs synthesized using CLS of *Vibrio* sp. VLC. The effects of CuO NP-1 (A, B) and CuO NP-2 (C, D) on *E. coli* and *S. aureus*. The results are shown as mean ± SD.

(IC_{50} = 27.70 mg/L for 72 h) (Fig. 10A). Data were expressed as means ± SD. Statistical analysis was performed using Student's *t*-test and differences were considered significant at $P \leq 0.05$.

We further analyzed several KYSE30 cells to determine CuO NPs distribution within the cells. According to TEM images (Fig. 11), CuO NPs were localized intracellularly in cytoplasm and organelles such as some vesicles, and nucleus (Fig. 11C), while there were not such nanoparticles in $CuSO_4$ treated cells (Fig. 11A). A small population of CuO NPs were also observed extracellularly very close to cytoplasmic membrane demonstrating a movement toward the cell interior (Fig. 11D).

3.5. Photoluminescence analysis

Fluorescent copper nanoparticles (F-CuNPs) have gained great attention due to their ease of functionalization and good biocompatibility. Fluorescent related approaches are also appropriate methods for sensing metal ions because of their low cost, high sensitivity, and ease of fabrication [33]. Photoluminescence spectra of CuO NPs with the excitation wavelength (λ_{ex}) of 310 nm are shown in Fig. 12(A–E). The maximum fluorescence emission intensity (F_{max}) was measured at 628 nm, when the NPs were dispersed in phosphate-buffered saline (PBS). The effects of heavy metals ions such as mercury (Hg^{2+}), lead (Pb^{2+}), arsenic (As^{2+}) and cadmium (Cd^{2+}) on fluorescence emission of CuO NPs showed that in presence of Cd^{2+}, As^{2+} and Hg^{2+} ions the fluorescence emission of CuO NPs increased but decreased in presence of Pb^{2+} ions (Fig. 12F–I).

4. Discussion

Metal resistance depends on several factors. The most common strategy for metal resistance among microbes is preventing the entry of metal into the cell and the second is the cell's ability to secure storage within the cells [19]. Microorganisms may decrease copper toxicity by reducing its salt ions to Cu^0. The highest metal concentration at which the bacteria can grow, was designated as the MTC. Rajaram and co-workers reported that among 12 isolates from the polluted coastal environment only 4 isolates showed high resistance to copper (up to 400–500 mg/L) [34]. Also, Andreazza and his co-workers evaluated the resistance of some bacteria isolated from the environment. Their results showed that only one isolate was able to absorb 80 mg/L of copper in 24 h [35]. *Vibrio* sp. VLC showed the highest resistance to 450 mg/L and as a marine isolate it was expected to see a fairly good resistance to copper.

Although several methods have been used to synthesize CuO NPs, in this study for the first time we applied a facile approach for the synthesis of CuO NPs by using a luminescent *Vibrio* species. It is assumed that cellular biomolecules such as enzymes and proteins present in the CLS reduce copper ions into copper atoms leading to CuO NPs formation. Harvested CLS in the stationary phase contains a high level of cellular enzymes and peripheral membrane proteins have an important role in higher efficiency of CuO NPs production. Accordingly, the reductase enzymes of luminescent bacteria were found to be involved in gold NPs biosynthesis [15]. In our study, only in the presence of CLS proteins was that high CuO NPs synthesis occurred which could strongly support the role of these proteins (both structural and enzymatic) in CuO NPs biosynthesis. Need to know that, there is not any

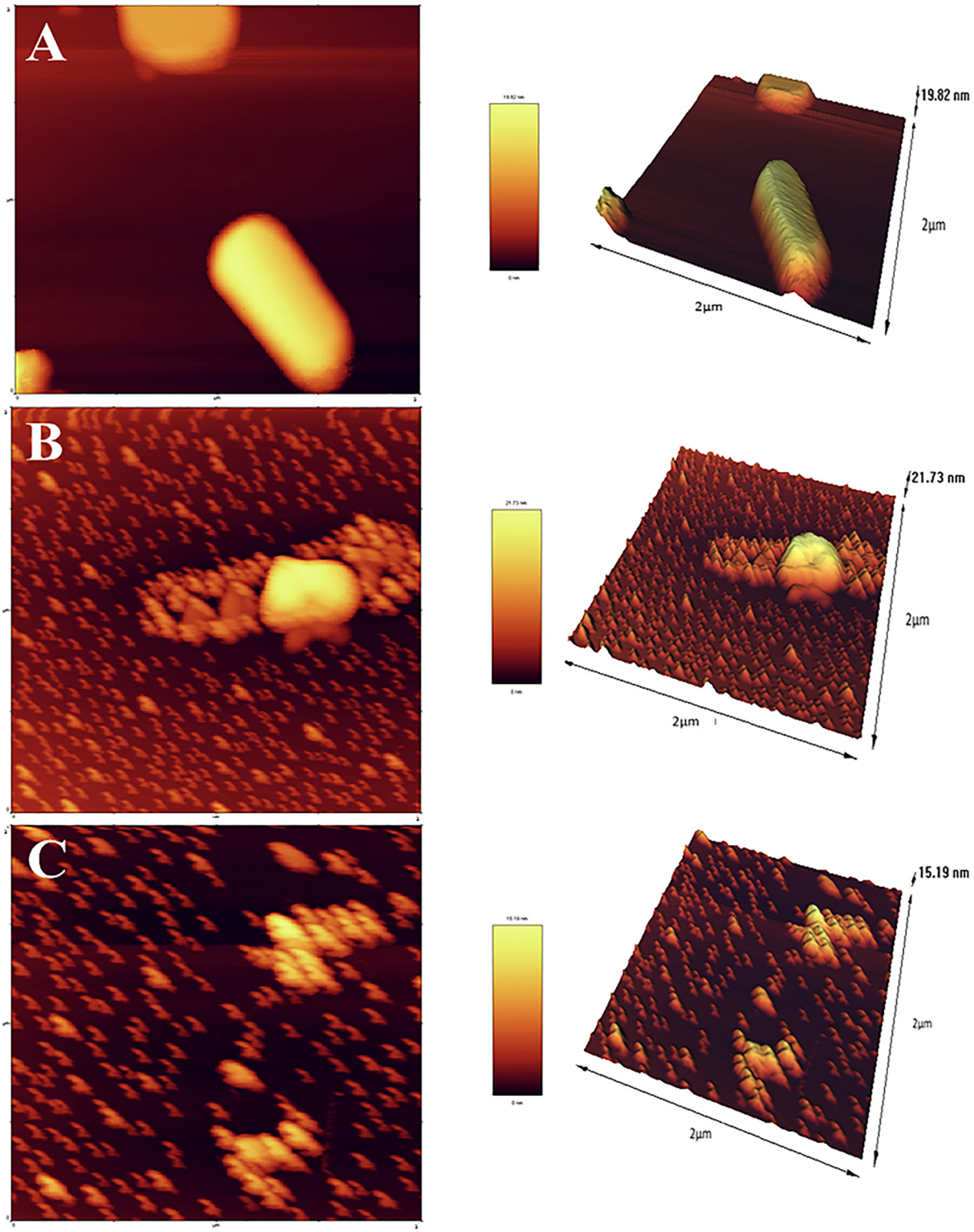

Fig. 9. AFM microscopic images; the effect of CuO NP-1 synthesized using CLS of *Vibrio* sp. VLC on the *E. coli*. A: control; B: 2 h after incubation; C: 6 h after incubation.

report indicating the application of proteins or even luminescent bacteria in CuO NPs production.

The position of UV peak depends on stability (pH, solvent type, stabilizing agent) shape and size of NPs [36]. Left shift observed in NPs UV spectrum can be related to the smaller size of NPs [37]. There are probably some factors in cell culture supernatant that play as stabilizing agents and could prevent NPs size enlargement. However, as CuO NPs synthesized by CLS method was bigger, it was easily removable by medium speed centrifugation. Therefore further characterization was performed on this sample. Shankar and Rhim used different types of copper salts and chemical reducing agents for CuO NPs synthesis reporting broad peaks around 280–360 nm in their UV–Vis spectrum analysis [30]. Also, CuO NPs synthesized by *Matricaria chamomilla* extract had broad peaks around 285 and 320 nm [37]. Results of these

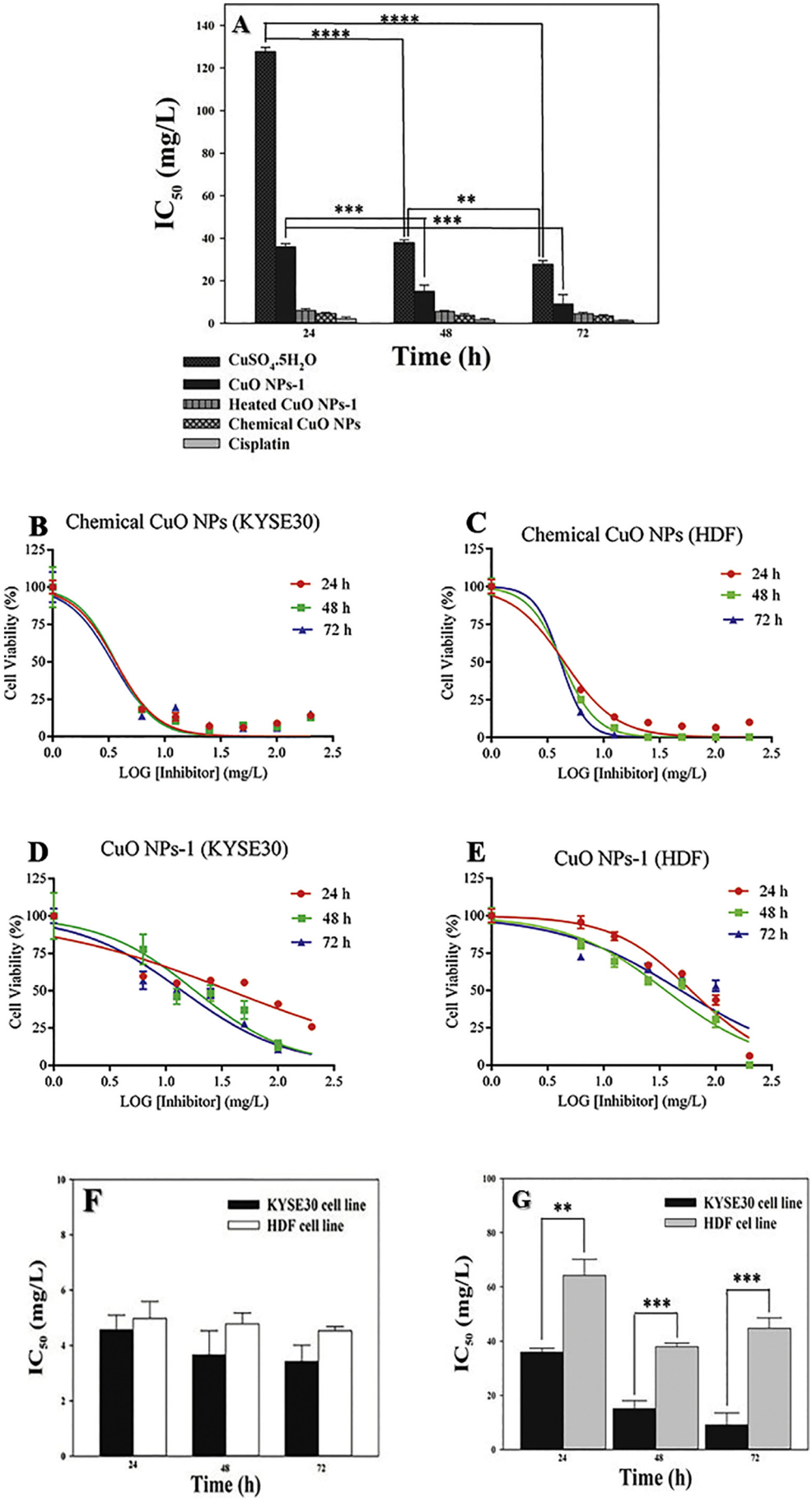

(caption on next page)

Fig. 10. CuO NP-induced cytotoxicity in KYSE30 cells (A). Dose-response curves representing the effects of chemical and biogenic CuO NPs on KYSE30 cells (B, D)/ HDF cells (C, E), at 24, 48 and 72 h intervals, respectively. Comparing the cytotoxicity of chemically synthesized (F) and biogenic CuO NPs-1 (G) on cancerous (dark color) and normal (light color) cells. Results are shown as mean ± SD. The difference between groups was analyzed using the Student's *t*-test. $^{**}P < 0.01$, $^{***}P < 0.001$ and $^{****}P < 0.0001$.

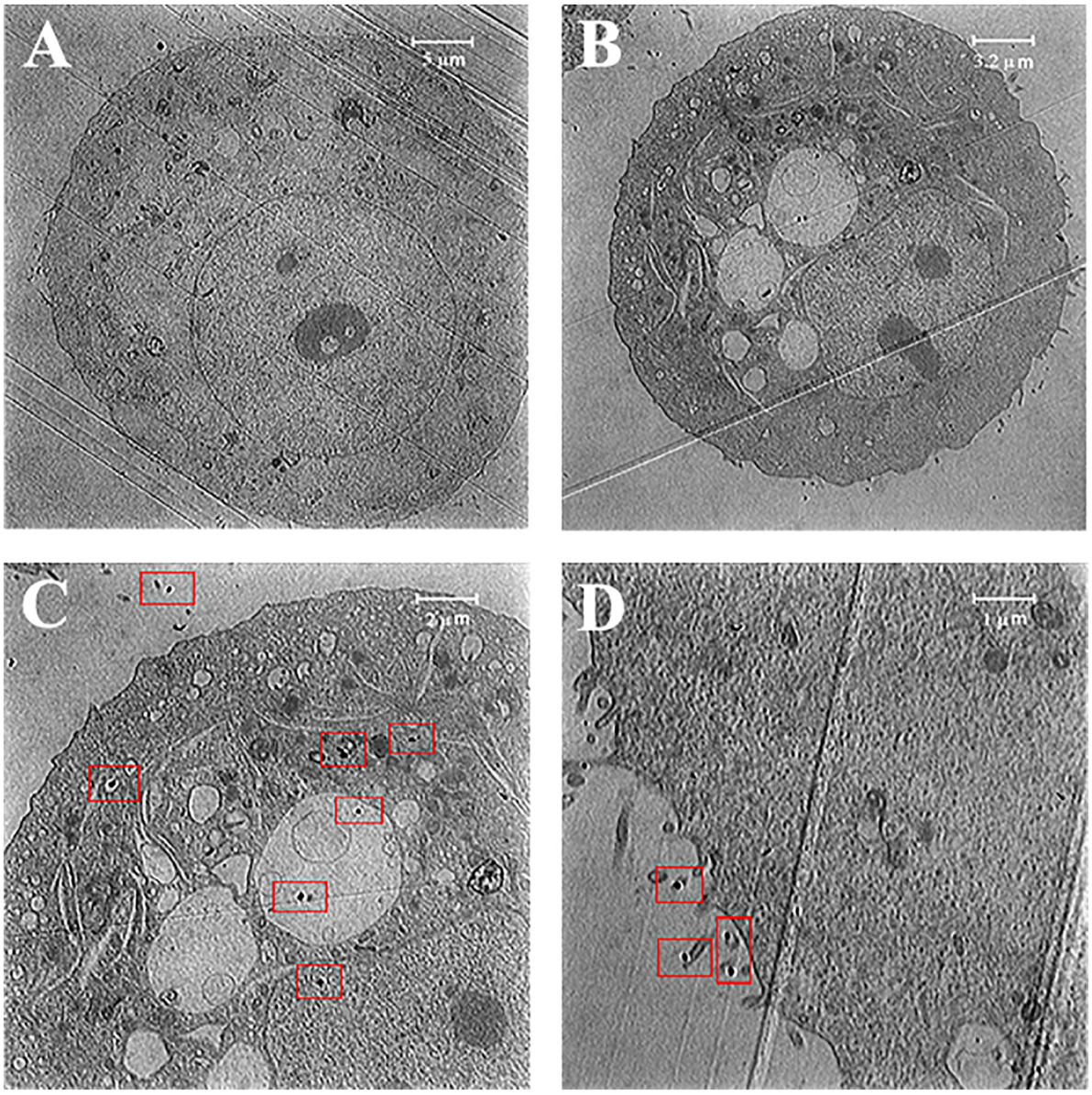

Fig. 11. TEM images of KYSE30 cells after exposure to $CuSO_4$ salt solutions (A) or CuO NPs-1 (B, C and D). C is an enlarged image showing CuO NPs presence in the cytoplasm, some vesicles and nucleus (red frames). D is also an enlarged image indicating the presences of CuO NPs outside the cell (red frames) in the stage of movement toward cell interior. (For interpretation of the references to color in this figure legend, the reader is referred to the web version of this article.)

studies were consistent with our results. Also in comparison Harne et al. and Duman et al. presented similar outcomes for their FTIR results [37,38]. Shankar & Rhim and Ahamed et al. reported a similar XRD pattern for CuO NPs in chemical reduction regime [30,31]. Similar XRD pattern was also found by Duman and co-workers when they used *Chamomile* extract with a microwave-assisted technique for their CuO NPs biosynthesis [37].

NPs antibacterial activity mostly depends on bacterial morphology as well as their nature [18,39]. Although NPs can attach to the membrane of bacteria interfering with bacterial membrane functions [40], many metal oxide NPs act differently on various bacterial strains. Also, parameters involved in mechanisms of NPs antibacterial activity could be affected by variations in the methodology resulting in lower or higher antimicrobial activity of NPs. MBC values for CuO NPs in Ren et al. study against *E. coli*, *P. aeruginosa* and *S. aureus* were 250, 5000 and 2500 mg/L, respectively [3]. Nabila and Kannabiran, biologically synthesized CuO NPs mediated by actinomycetes but the average size of their biogenic CuO NPs according to XRD and TEM analyses was 61.7 nm larger than our luminescent *Vibrio* mediated synthesized CuO NPs (8.83 nm) [41]. The properties of most nanoparticles have been found to be size-dependent as highly stable minimum-sized monodispersed CuO NPs synthesized in Azam et al. studies demonstrated a significant increase in antibacterial activities against both Gram-positive and Gram-negative bacterial strains [42].

In comparison, our CuO NPs had a better bactericidal effect on the *P. aeruginosa* and *S. aureus*. Usually, DIZ of gram-negative bacteria is

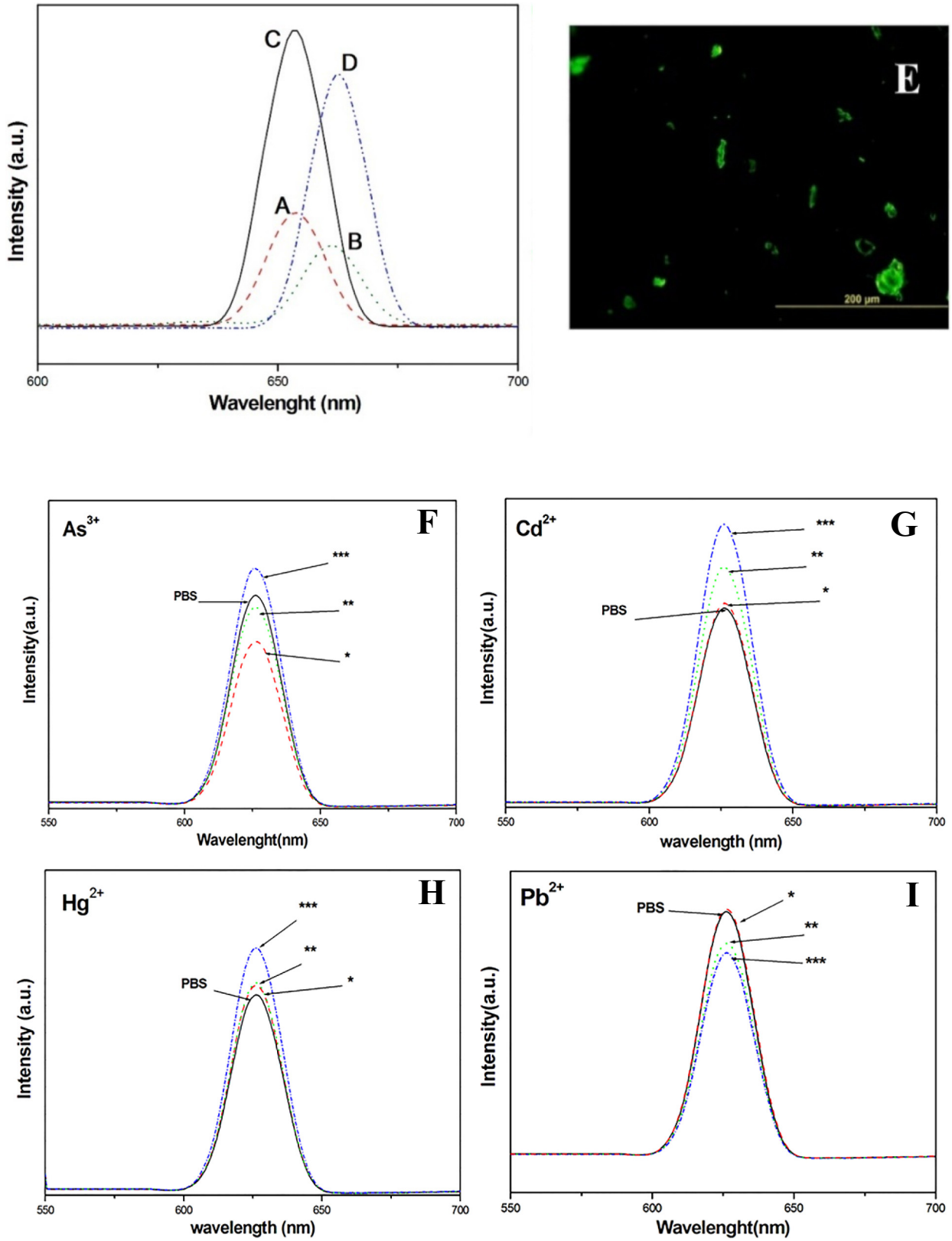

Fig. 12. Fluorescent spectroscopy diagram (A, B, C and D) and microscopy image (E) of CuO NP-2 synthesized using CLS of *Vibrio* sp. VLC, A: solvent distilled water; B: solvent ethanol; C: solvent PBS; D: solvent RPMI medium. Effect of different concentrations (10(*), 100(**), 1000(***) times of limit value set by the World Health Organization) of heavy metals (F: As^{3+}, G: Cd^{2+}, H: Hg^{2+}, and I: Pb^{2+}) on the emission spectrum of biogenic CuO NPs-2 synthesized using CLS of *Vibrio* sp. VLC.

smaller than gram-positive bacteria mostly due to outer membrane presence in gram-negative bacteria that prevent penetration of anti-bacterial agents [39]. Several mechanisms can be proposed for antimicrobial effects of present CuO NPs on tested bacterial cells such as (i) releasing of copper ions, (ii) production of reactive oxygen species (ROS) and (iii) binding NPs to the surface of bacteria [43]. The

antibacterial activity of our prepared CuO NPs was very close to the results of Laha and co-workers when they treated the *E. coli* with CuO NPs and nanosheets [39]. Altogether the methodology established in this study for protein-mediated CuO NPs biosynthesis seems to be effective on CuO NPs antibacterial activity.

CuO NPs-induced toxicity in a cell specific manner has been investigated in several cancer cell lines. Shafagh et al. found that CuO NPs exert distinct effects on cell viability via selective killing of human K562 cancer cells in a dose-dependent manner while not impacting normal cells as determined by MTT assay [44]. Similarly, our biogenic CuO NPs exhibited a dose-dependent cytotoxicity effect with the privilege of being safer in production and usage. Sankar and his co-workers also reported that cell viability of A549 human lung cancer cells decreased significantly [IC_{50} = 200 mg/L (36 h)] when exposed to CuO NPs produced by *Ficus religiosa* leaf extract [45]. This shows our CuO NPs have higher cancer cell cytotoxicity effects. Meanwhile, the effectiveness of heated CuO NP-1 on KYSE30 cell viability [IC_{50} = 4.44 mg/L (72 h)] was approximately similar to that of chemically synthesized CuO NPs [IC_{50} = 3.43 mg/L (72 h)]. This might be due to the presence of bioactive molecules in CLS content which plays as encapsulating agents for CuO NPs. Our prepared polydispersed CuO NPs showed higher cytotoxicity efficiency than copper salt (CuSO4.5H2O). Thit et al. found that polydispersed CuO NPs were more effective on A6 cancer cells (derived from the kidney of the *Xenopus laevis*) than 6 nm CuO NPs and Copper (Cu) ions administered as $CuCl_5.2H_2O$ [46], their reports were close to our results. Several mechanisms are suggested for cytotoxic effects of NPs on cancer cells like the production of reactive oxygen species (ROS) that causes DNA damage followed by cell death mainly via apoptosis [45,47,48]. Gunawan and co-workers pointed out that copper salts were able to release large quantities of metal ions in the medium that are toxic to cancer cells [47]. In another research, the release of Cu (II) cations and shape of these CuO NPs are likely to be implicated in the toxicity of these CuO NPs [49]. The morphologies, ion release rate of CuNPs, as well as the species-specific vulnerabilities of cells, should all be considered when extrapolating toxicity test results among particles and among different cell lines [50]. Meanwhile, no other associated factors such as bacterial cell wall components (lipidA) could interfere with the results of our CuO NPs cell cytotoxicity because of the methods used for NPs biosynthesis (CLS) and preparation. However, in our study $CuSO_4.5H_2O$ had less cytotoxic effects regardless of its high ability to release metal ions which agrees with studies of Wang et al. [51]. Moreover, Thit and co-workers suggested that high toxicity of polydispersed CuO NPs to cancer cells could be more related to high sedimentation of these polydispersed NPs [48]. A similar mechanism can be considered for anticancer properties of CuO NP-1 but further evidence has to be provided for confirmation. Furthermore, TEM analysis demonstrated CuO NP entry into KYSE30 cells and organelles, including some vesicles and nucleus. The results confirm uptake of CuO NPs compared to no uptake of the soluble salts ($CuSO_4$). Therefore, CuO NPs can induce both cell death and DNA damage to cancerous KYSE30 cells whereas $CuSO_4$ induces either low or no cytotoxicity. CuO NPs cytotoxicity is predominantly mediated by intracellular uptake and subsequent release of copper ions [52].

The application of F—Cu NPs as a biosensor has been mentioned in several pieces of literature [33,53–55]. The synthesis of CuO NPs in our study has been easy, fast and eco-friendly, whereas other methods needed a special ligand [33]. Generally, the detection mechanism for metal ions using F-CuO NPs is mainly composed of (i) fluorescence turn-off, (ii) fluorescence turn-on, (iii) fluorescence resonance energy transfer (FRET) and (iv) ratiometric response [54]. The fluorescence of CuO NPs increased in presence of Cd^{2+}, As^{2+} and Hg^{2+} ions and decreased in presence of Pb^{2+} ions. As changes were concentration-dependent confirmed previous conclusions that quenching and increasing of fluorescence emission could be related to interactions between metal ions and biological agents on the surface of nanoparticle [33,53–55]. Because of this property, our biogenic nanoparticle was being functional at heavy metal sensing activities in industrial. (i) Synthesis method, (ii) type of ligand, (iii) aggregation patterns and (iv) stabilizing agents could have significant effects on the fluorescence properties of fluorescent CuO NPs (F-CuO NP) [33,53].

5. Conclusion

In this study, novel non-toxic approaches for the production of CuO NPs (CLS method) were used. Moreover, the role of proteins in the reduction of Cu ions to CuO NPs was investigated. CuO NPs purification using this method was very convenient and fast which is quite advantageous over other methods, especially for its further industrialization and commercialization. CuO NPs emitted fluorescence light without the addition of any excess ligands to the synthetic route and were used to detect heavy metal ions in defined samples. Additionally, CuO NP-1 had suitable cytotoxic effects on KYSE30 esophageal cancer cells demonstrating its potent anticancer applications. Furthermore, the antibacterial activity of CuO NP-1 against certain microbial pathogens was confirmed indicating multifunctional properties of present CuO NPs.

Acknowledgments

We acknowledge financial support from Ferdowsi University of Mashhad (grant number: 3/41278).

References

[1] R. Dastjerdi, M. Montazer, A review on the application of inorganic nano-structured materials in the modification of textiles: focus on anti-microbial properties, Colloids Surf. B: Biointerfaces 79 (2010) 5–18, https://doi.org/10.1016/j.colsurfb.2010.03.029.

[2] K. Delgado, R. Quijada, R. Palma, H. Palza, Polypropylene with embedded copper metal or copper oxide nanoparticles as a novel plastic antimicrobial agent, Lett. Appl. Microbiol. 53 (2011) 50–54, https://doi.org/10.1111/j.1472-765X.2011.03069.x.

[3] G. Ren, D. Hu, E.W.C. Cheng, M.A. Vargas-Reus, P. Reip, R.P. Allaker, Characterisation of copper oxide nanoparticles for antimicrobial applications, Int. J. Antimicrob. Agents 33 (2009) 587–590, https://doi.org/10.1016/j.ijantimicag.2008.12.004.

[4] S. Luo, F. Su, C. Liu, J. Li, R. Liu, Y. Xiao, Y. Li, X. Liu, Q. Cai, A new method for fabricating a CuO/TiO2 nanotube arrays electrode and its application as a sensitive nonenzymatic glucose sensor, Talanta 86 (2011) 157–163, https://doi.org/10.1016/j.talanta.2011.08.051.

[5] D. Rehana, D. Mahendiran, R.S. Kumar, A.K. Rahiman, Evaluation of antioxidant and anticancer activity of copper oxide nanoparticles synthesized using medicinally important plant extracts, Biomed. Pharmacother. 89 (2017) 1067–1077, https://doi.org/10.1016/j.biopha.2017.02.101.

[6] M. Roy Chowdhury, C. Schumann, D. Bhakta-Guha, G. Guha, Cancer nanotheranostics: strategies, promises and impediments, Biomed. Pharmacother. 84 (2016) 291–304, https://doi.org/10.1016/j.biopha.2016.09.035.

[7] G.G. Jang, C.B. Jacobs, R.G. Gresback, I.N. Ivanov, H.M. Meyer, III, M. Kidder, P.C. Joshi, G.E. Jellison, T.J. Phelps, D.E. Graham, J.-W. Moon, Size tunable elemental copper nanoparticles: extracellular synthesis by thermoanaerobic bacteria and capping molecules, J. Mater. Chem. C 3 (2015) 644–650, https://doi.org/10.1039/C4TC02356K.

[8] A.V. Tugarova, A.A. Kamnev, Proteins in microbial synthesis of selenium nanoparticles, Talanta 174 (2017) 539–547, https://doi.org/10.1016/j.talanta.2017.06.013.

[9] R.C. Kasana, N.R. Panwar, R.K. Kaul, P. Kumar, Biosynthesis and effects of copper nanoparticles on plants, Environ. Chem. Lett. 15 (2017) 233–240, https://doi.org/10.1007/s10311-017-0615-5.

[10] S. Saif Hasan, S. Singh, R.Y. Parikh, M.S. Dharne, M.S. Patole, B.L.V. Prasad, Y.S. Shouche, Bacterial synthesis of copper/copper oxide nanoparticles, J. Nanosci. Nanotechnol. 8 (2008) 3191–3196, https://doi.org/10.1166/jnn.2008.095.

[11] H.R. Ghorbani, Extracellular synthesis of copper nanoparticles using culture supernatants of Salmonella typhimurium, Orient. J. Chem. 31 (2015) 527–529, https://doi.org/10.13005/ojc/310165.

[12] A. V. Singh, R. Patil, A. Anand, P. Milani, W.N. Gade, Biological synthesis of copper oxide nano particles using Escherichia coli, Curr. Nanosci. 6 (2010) 365–369, https://doi.org/10.2174/157341310791659062.

[13] J. Tiwari, M. Narayanan, K. Thakar, M.B. Jagani, H.V. Rao, Biosynthesis and wound healing activity of copper nanoparticles, IET Nanobiotechnol. 8 (2014) 230–237, https://doi.org/10.1049/iet-nbt.2013.0052.

[14] V. Ramanathan, R. Field, M. O'Mullane, A.P. Smooker, P.M. Bhargavabc, S.K. Bansal, Aqueous phase synthesis of copper nanoparticles: a link between heavy metal resistance and nanoparticle synthesis ability in bacterial systems, Nanoscale 5

(2013) 2300–2306, https://doi.org/10.1039/C2NR32887A.
[15] M. Hosseini, M. Mashreghi, H. Eshghi, Biosynthesis and antibacterial activity of gold nanoparticles coated with reductase enzymes, Micro Nano Lett 11 (2016) 484–489.
[16] M. Attaran, N. Eshghi, H. Rahimizadeh, M. Mashreghi, M. Bakavoli, Genetically modified luminescent bacteria Ralostonia solanacerum, Pseudomonas syringae, Pseudomonas savastanoi, and wild type bacterium Vibrio fischeri in biosynthesis of gold nanoparticles from gold chloride trihydrate, Artif. Cells, Nanomedicine, Biotechnol. 44 (2016) 263–269, https://doi.org/10.3109/21691401.2014.942457.
[17] M. Masoudi, M. Mashreghi, E. Goharshadi, A. Meshkini, Multifunctional fluorescent titania nanoparticles: green preparation and applications as antibacterial and cancer theranostic agents, Artif. Cells, Nanomedicine, Biotechnol. (2018) 1–12, https://doi.org/10.1080/21691401.2018.1454932.
[18] Y.N. Tan, J.Y. Lee, D.I.C. Wang, Uncovering the design rules for peptide synthesis of metal nanoparticles, J. Am. Chem. Soc. 132 (2010) 5677–5686, https://doi.org/10.1021/ja907454f.
[19] S. Shakya, B. Pradhan, L. Smith, J. Shrestha, S. Tuladhar, Isolation and characterization of aerobic culturable arsenic-resistant bacteria from surfacewater and groundwater of Rautahat District, Nepal, J. Environ. Manag. 95 (2012) S250–S255, https://doi.org/10.1016/j.jenvman.2011.08.001.
[20] S. Singh, A.S. Vidyarthi, V.K. Nigam, A. Dev, Extracellular facile biosynthesis, characterization and stability of gold nanoparticles by Bacillus licheniformis, Artif. Cells, Nanomedicine, Biotechnol. 42 (2014) 6–12, https://doi.org/10.3109/21691401.2012.759122.
[21] S. Zerbs, A.M. Frank, F.R. Collart, Chapter 12 Bacterial Systems for Production of Heterologous Proteins, (2009), pp. 149–168, https://doi.org/10.1016/S0076-6879(09)63012-3.
[22] S. Dehghanizade, J. Arasteh, A. Mirzaie, Green synthesis of silver nanoparticles using Anthemis atropatana extract: characterization and in vitro biological activities, Artif. Cells, Nanomedicine, Biotechnol. 46 (2018) 160–168, https://doi.org/10.1080/21691401.2017.1304402.
[23] J.M. Andrews, Determination of minimum inhibitory concentrations, J. Antimicrob. Chemother. 48 (2001) 5–16, https://doi.org/10.1093/jac/48.suppl_1.5.
[24] M.A. Adahoun, M.-A.H. Al-Akhras, M.S. Jaafar, M. Bououdina, Enhanced anticancer and antimicrobial activities of curcumin nanoparticles, Artif. Cells, Nanomedicine, Biotechnol. 45 (2017) 98–107, https://doi.org/10.3109/21691401.2015.1129628.
[25] M. Dowlatabadi, F.H. Amiri, G.M. Sichani, Investigation of the antimicrobial effect of silver doped zinc oxide nanoparticles, Nanomedicine J. 4 (2017) 50–54.
[26] B.-J. Chen, N.S. Jamaludin, C.-H. Khoo, T.-H. See, J.-H. Sim, Y.-K. Cheah, S.N.A. Halim, H.-L. Seng, E.R.T. Tiekink, In vitro antibacterial and time kill evaluation of mononuclear phosphanegold(I) dithiocarbamates, J. Inorg. Biochem. 163 (2016) 68–80, https://doi.org/10.1016/j.jinorgbio.2016.08.002.
[27] M. GAD, Mapping cell wall polysaccharides of living microbial cells using atomic force microscopy, Cell Biol. Int. 21 (1997) 697–706, https://doi.org/10.1006/cbir.1997.0214.
[28] C. Wang, Z. Li, F. Shao, X. Yang, X. Feng, S. Shi, Y. Gao, J. He, High expression of Collagen Triple Helix Repeat Containing 1 (CTHRC1) facilitates progression of oesophageal squamous cell carcinoma through MAPK/MEK/ERK/FRA-1 activation, J. Exp. Clin. Cancer Res. 36 (2017) 84, , https://doi.org/10.1186/s13046-017-0555-8.
[29] L. Qiu, G. Lv, Y. Cao, L. Chen, H. Yang, S. Luo, M. Zou, J. Lin, Synthesis and biological evaluation of novel platinum complexes of imidazolyl-containing bisphosphonates as potential anticancer agents, JBIC, J. Biol. Inorg. Chem. 20 (2015) 1263–1275, https://doi.org/10.1007/s00775-015-1305-z.
[30] S. Shankar, J.-W. Rhim, Effect of copper salts and reducing agents on characteristics and antimicrobial activity of copper nanoparticles, Mater. Lett. 132 (2014) 307–311, https://doi.org/10.1016/j.matlet.2014.06.014.
[31] M. Ahamed, H.A. Alhadlaq, M.A.M. Khan, P. Karuppiah, N.A. Al-Dhabi, Synthesis, characterization, and antimicrobial activity of copper oxide nanoparticles, J. Nanomater. 2014 (2014) 1–4, https://doi.org/10.1155/2014/637858.
[32] C.Y. Tay, M.I. Setyawati, J. Xie, W.J. Parak, D.T. Leong, Back to basics: exploiting the innate physico-chemical characteristics of nanomaterials for biomedical applications, Adv. Funct. Mater. 24 (2014) 5936–5955, https://doi.org/10.1002/adfm.201401664.
[33] Y. Guo, F. Cao, X. Lei, L. Mang, S. Cheng, J. Song, Fluorescent copper nanoparticles: recent advances in synthesis and applications for sensing metal ions, Nanoscale 8 (2016) 4852–4863, https://doi.org/10.1039/C6NR00145A.
[34] R. Rajaram, J.S. Banu, K. Mathivanan, Biosorption of Cu (II) ions by indigenous copper-resistant bacteria isolated from polluted coastal environment, Toxicol. Environ. Chem. 95 (2013) 590–604, https://doi.org/10.1080/02772248.2013.801979.
[35] R. Andreazza, S. Pieniz, L. Wolf, M.-K. Lee, F.A.O. Camargo, B.C. Okeke, Characterization of copper bioreduction and biosorption by a highly copper resistant bacterium isolated from copper-contaminated vineyard soil, Sci. Total Environ. 408 (2010) 1501–1507, https://doi.org/10.1016/j.scitotenv.2009.12.017.
[36] J. Díaz-Visurraga, Daza, C. Pozo Valenzuela, Becerra, A. García Cancino, C. von Plessing, Study on antibacterial alginate-stabilized copper nanoparticles by FT-IR and 2D-IR correlation spectroscopy, Int. J. Nanomedicine (2012) 3597, https://doi.org/10.2147/IJN.S32648.
[37] F. Duman, I. Ocsoy, F.O. Kup, Chamomile flower extract-directed CuO nanoparticle formation for its antioxidant and DNA cleavage properties, Mater. Sci. Eng. C 60 (2016) 333–338, https://doi.org/10.1016/j.msec.2015.11.052.
[38] S. Harne, A. Sharma, M. Dhaygude, S. Joglekar, K. Kodam, M. Hudlikar, Novel route for rapid biosynthesis of copper nanoparticles using aqueous extract of Calotropis procera L. latex and their cytotoxicity on tumor cells, Colloids Surf. B: Biointerfaces 95 (2012) 284–288, https://doi.org/10.1016/j.colsurfb.2012.03.005.
[39] D. Laha, A. Pramanik, A. Laskar, M. Jana, P. Pramanik, P. Karmakar, Shape-dependent bactericidal activity of copper oxide nanoparticle mediated by DNA and membrane damage, Mater. Res. Bull. 59 (2014) 185–191, https://doi.org/10.1016/j.materresbull.2014.06.024.
[40] A. Nayamadi Mahmoodabadi, A. Kompany, M. Mashreghi, Characterization, antibacterial and cytotoxicity studies of graphene-Fe3O4 nanocomposites and Fe3O4 nanoparticles synthesized by a facile solvothermal method, Mater. Chem. Phys. 213 (2018) 285–294, https://doi.org/10.1016/j.matchemphys.2018.04.033.
[41] M.I. Nabila, K. Kannabiran, Biosynthesis, characterization and antibacterial activity of copper oxide nanoparticles (CuO NPs) from actinomycetes, Biocatal. Agric. Biotechnol. 15 (2018) 56–62, https://doi.org/10.1016/j.bcab.2018.05.011.
[42] A. Azam, Size-dependent antimicrobial properties of CuO nanoparticles against Gram-positive and -negative bacterial strains, Int. J. Nanomedicine (2012) 3527, https://doi.org/10.2147/IJN.S29020.
[43] Y. Li, W. Zhang, J. Niu, Y. Chen, Surface-coating-dependent dissolution, aggregation, and reactive oxygen species (ROS) generation of silver nanoparticles under different irradiation conditions, Environ. Sci. Technol. (2013) 130904083900006, , https://doi.org/10.1021/es400945v.
[44] M. Shafagh, F. Rahmani, N. Delirezh, CuO nanoparticles induce cytotoxicity and apoptosis in human K562 cancer cell line via mitochondrial pathway, through reactive oxygen species and P53, Iran. J. Basic Med. Sci. 18 (2015) 993.
[45] R. Sankar, R. Maheswari, S. Karthik, K.S. Shivashangari, V. Ravikumar, Anticancer activity of Ficus religiosa engineered copper oxide nanoparticles, Mater. Sci. Eng. C 44 (2014) 234–239, https://doi.org/10.1016/j.msec.2014.08.030.
[46] A. Thit, H. Selck, H.F. Bjerregaard, Toxicity of CuO nanoparticles and Cu ions to tight epithelial cells from Xenopus laevis (A6): effects on proliferation, cell cycle progression and cell death, Toxicol. in Vitro 27 (2013) 1596–1601, https://doi.org/10.1016/j.tiv.2012.12.013.
[47] C. Gunawan, W.Y. Teoh, C.P. Marquis, R. Amal, Cytotoxic origin of copper(II) oxide nanoparticles: comparative studies with micron-sized particles, leachate, and metal salts, ACS Nano 5 (2011) 7214–7225, https://doi.org/10.1021/nn2020248.
[48] A. Thit, H. Selck, H.F. Bjerregaard, Toxic mechanisms of copper oxide nanoparticles in epithelial kidney cells, Toxicol. in Vitro 29 (2015) 1053–1059, https://doi.org/10.1016/j.tiv.2015.03.020.
[49] J.-P. Piret, S. Vankoningsloo, J. Mejia, F. Noël, E. Boilan, F. Lambinon, C.C. Zouboulis, B. Masereel, S. Lucas, C. Saout, O. Toussaint, Differential toxicity of copper (II) oxide nanoparticles of similar hydrodynamic diameter on human differentiated intestinal Caco-2 cell monolayers is correlated in part to copper release and shape, Nanotoxicology 6 (2012) 789–803, https://doi.org/10.3109/17435390.2011.625127.
[50] L. Song, M. Connolly, M.L. Fernández-Cruz, M.G. Vijver, M. Fernández, E. Conde, G.R. de Snoo, W.J.G.M. Peijnenburg, J.M. Navas, Species-specific toxicity of copper nanoparticles among mammalian and piscine cell lines, Nanotoxicology 8 (2014) 383–393, https://doi.org/10.3109/17435390.2013.790997.
[51] Z. Wang, N. Li, J. Zhao, J.C. White, P. Qu, B. Xing, CuO nanoparticle interaction with human epithelial cells: cellular uptake, location, export, and genotoxicity, Chem. Res. Toxicol. 25 (2012) 1512–1521, https://doi.org/10.1021/tx3002093.
[52] P. Cronholm, H.L. Karlsson, J. Hedberg, T.A. Lowe, L. Winnberg, K. Elihn, I.O. Wallinder, L. Möller, Intracellular uptake and toxicity of Ag and CuO nanoparticles: a comparison between nanoparticles and their corresponding metal ions, Small 9 (2013) 970–982, https://doi.org/10.1002/smll.201201069.
[53] A. Rotaru, S. Dutta, E. Jentzsch, K. Gothelf, A. Mokhir, Selective dsDNA-templated formation of copper nanoparticles in solution, Angew. Chem. Int. Ed. 49 (2010) 5665–5667, https://doi.org/10.1002/anie.200907256.
[54] Y. Guo, L. Zhang, S. Zhang, Y. Yang, X. Chen, M. Zhang, Fluorescent carbon nanoparticles for the fluorescent detection of metal ions, Biosens. Bioelectron. 63 (2015) 61–71, https://doi.org/10.1016/j.bios.2014.07.018.
[55] Y. Guo, Z. Wang, H. Shao, X. Jiang, Hydrothermal synthesis of highly fluorescent carbon nanoparticles from sodium citrate and their use for the detection of mercury ions, Carbon N. Y. 52 (2013) 583–589, https://doi.org/10.1016/j.carbon.2012.10.028.